Experimental Determination of Damping Mechanisms in a Composite Beam

H.T. Banks
Center for Control Sciences
Division of Applied Mathematics
Brown University
Providence, Rhode Island 02912

D.J. Inman
Department of Mechanical and Aerospace Engineering
State University of New York at Buffalo
Buffalo, New York 14260

Abstract

A partial differential equation model of a cantilevered beam with a tip mass at its free end is used to study damping in a composite. Four separate damping mechanisms consisting of air damping, strain rate damping, spatial hysteresis and time hysteresis are considered experimentally. Dynamic tests were performed to produce time histories. The time history data is then used along with an approximate model to form a sequence of least squares problems. The solution of the least squares problem yields the estimated damping coefficients. The resulting experimentally determined analytical model is compared with the time histories via numerical simulation of the dynamic response. The procedure suggested here is compared with a standard modal damping ratio model commonly used in experimental modal analysis.

I. Introduction

This paper examines a variety of damping mechanisms of a quasi-isotropic pultruded composite beam. The approach taken here is a physical one. The beam is modeled by a partial differential equation describing the transverse vibration of a beam with tip mass. The damping mechanisms considered are all physically based rather then the usual modal models. In total, four possible damping mechanisms are considered, one external and three internal. They are:

- viscous damping (air damping)
- strain rate damping
- spatial hysteresis
- time hysteresis

In addition, various combinations of these mechanisms are considered. These physical damping models are incorporated into the Euler-Bernoulli beam equation, taking care to adjust the boundary conditions for the various damping forces. The resulting partial differential equation is approximated using cubic splines. The time histories of the measured experimental responses are then used to form a least squares fit-to-data parameter estimation problem. The mathematical details for this procedure are complete and imply convergence of a sequence of parameter estimates obtained from finite dimensional models to a set of best fit coefficients of the partial differential equation model. The least square estimates of the various different damping parameters are then used in the partial differential/integral equation to numerically predict the response of the system. This numerically generated time response of the estimated system is then compared with the actual experimental time histories. These comparisons allow several conclusions to be drawn regarding the physical damping mechanisms present in the composite beam.

In particular it is shown that the spatial hysteresis model combined with a viscous air damping model results in the best reproduction of experimental time histories. The results agree well with the physically intuitive notion that air damping should play a more significant role in lower modes while internal damping plays a more significant role for higher modes. It is also shown explicitly that the proposed damping models listed above cannot be modeled with any degree of success or consistency by using standard modal damping ratios, as the traditional modal analysis approach completely masks the physics of damping mechanisms.

II. Basic Beam Model

The beam considered here is a pultruded quasi-isotropic composite beam constructed for use in the proposed space station.[1] As such, the configuration of interest is a cantilevered beam with a mass attached to the free end. The beam is constructed of a biaxial ($0^\circ/90^\circ$) fiberglass roving held in place with knitted polyester yarn with an equal volume of fibre in both orientations. An isophtalic polyester resin system was used as the matrix. This material provides an alternative to aluminum which is lower in cost, has higher specific strength but is dynamically similar. As is illustrated here, this material also has interesting damping properties - dissimilar to those of aluminum.

The equation of motion for the flexual vibration of a beam is easily calculated from considering the equilibrium of forces acting on a differential segment of beam (see for instance Reference 2). In this formulation, damping can easily be included by adding the appropriate force or moment to the equations of equilibrium. A general partial differential equation model of the beam with general damping is of the form

$$u_{tt}(x,t) + L_1 u_t(x,t) + L_2 u(x,t) \frac{\partial^2}{\partial x^2} + \left[\frac{EI(x)}{\rho A} u_{xx}(x,t) \right] = f(x,t) \qquad (1)$$

for $x \in (0, l)$, $t > 0$, subject to the appropriate boundary and initial conditions (taken to be $u = u_t = 0$ at $t = 0$). Here ρ is the mass density (mass per unit length) of the beam, A is the cross sectional area of the beam, $EI(x)$ is the spatial varying flexural stiffness of the beam, the subscript indicates partial differentiation with respect to the indicated variable and $u(x,t)$ is the beam displacement in the transverse direction. The function $u(x,t)$ is assumed to be smooth enough so that all the appropriate derivatives exist. The term $L_1 u_t(x,t) + L_2 u(x,t)$ forms the subject of this paper. The nature of the operator L_1 is determined by the external damping mechanisms while the nature of the term $L_2 u(x,t)$ is determined by internal damping mechanisms.

The boundary conditions of interest here are those for a beam clamped at the end $x = 0$ and with a free end at $x = l$. Also at $x = l$, a mass of mass m_T and rotational inertia J, resides. The fixed end requires that the displacement and the slope of the displacement both be zero. This yields:

$$u(0,t) = 0 \tag{2}$$

$$u_x(0,t) = 0 \tag{3}$$

The free end requires that the sum of the moments at $x = l$ and the sum of the forces acting at $x = l$ must both be zero. For the case of a tip mass at the free end, these boundary conditions become

$$EI(l)u_{xx}(l,t) = -J\,u_{ttx}(l,t) \tag{4}$$

$$[EI(l)u_{xx}(l,t)]_x = m_T u_{tt}(l,t) \tag{5}$$

as long as only external damping is present.

Equations (1) - (5) describe the transverse vibration of a beam satisfying the Bernoulli-Euler assumption that the bending wave length is several times larger than the cross sectional dimensions of the beam, and that only lower frequency excitations are applied to the beam. It is also assumed that rotary inertia of the beam, shear displacement of the beam and axial displacements are negligible.

If the tip mass is not present, the boundary conditions of equations (4) and (5) change accordingly. In addition, the nature of the damping operator L_2 will effect the boundary conditions. For the case of $L_1 = L_2 = 0$, the vibration analysis problem is very simple as is the inverse problem addressed here. The nature of the damping mechanisms drastically changes the nature of the solution to the vibration problem and hence controls the response of the beam. The following section discusses several possible choices for modeling the operator L_2 in equation (1) and hence the damping mechanisms.

III. Damping Models

As mentioned in the introduction four models of the damping mechanism are examined. Two of these are time independent proportional models lending themselves to modal expansions, the other two are nonproportional hysteretic models. Various combinations of these models are also considered.

Viscous Air Damping The most straight forward method of modeling the damping of a beam (or other object) vibrating in air is to use a viscous model proportional to velocity. In this case the operator L_1 becomes

$$L_1 = \gamma I_0 \tag{6}$$

where I_0 is the identity operator and γ is the viscous damping constant of proportionality. The physical basis of this approach is a sample model of air resistance. As the beam vibrates it must displace air causing the force $\gamma u_t(x,t)$ to be applied to the beam. Mathematically, this form of damping is used because it is proportional and easily treated using the same methods of analysis used for undamped systems (see Reference 3 for instance). Both experimental modal analysis and

theoretical modal analysis depend on the validity of these models. This form of damping is often called external damping.

Kelvin-Voight Damping Kelvin-Voight damping, or strain rate damping as it is sometimes called, is damping of the form

$$L_2 = c_d I \frac{\partial^5}{\partial x^4 \partial t} \tag{7}$$

where I is the moment of inertia and c_d is the strain rate damping coefficient or strain velocity. This model also satisfies a proportional damping criteria and hence is mathematically convenient. This model is compatible with theoretical modal analysis and is also widely used in finite element modeling along with viscous damping. Physically, this form of damping is referred to as internal damping and represents energy dissipated by friction internal to the beam.

Unlike viscous external damping, inclusion of this form of damping affects the free end boundary conditions because it is strain dependent. The strain rate dependance results in a damping moment M_D of the form

$$M_D = c_d I(x) \frac{\partial^3 u}{\partial x^2 \partial t} \tag{8}$$

which is included in the derivation of the equation of motion[2] and hence must also be included in any boundary conditions (such as a free end condition) depending on the moment.

The full equation of motion and boundary conditions for the linear viscously damping case becomes

$$\begin{aligned}
&\rho u_{tt} + \frac{\partial^2}{\partial x^2}[EIu_{xx}] + c_d I u_{xxxxt} + \gamma u_t = f(x,t) \qquad x \in (0,l), \quad t > 0 \\
&u(0,t) = u_x(0,t) = 0 \ , \qquad t > 0 \\
&EIu_{xx}(l,t) + c_d I \frac{\partial^3}{\partial x^2 \partial t} u(l,t) = -Ju_{xtt}(l,t) \ , \qquad t > 0 \\
&\frac{\partial}{\partial x}[EIu_{xx}(l,t)] + \frac{\partial}{\partial x}[c_d I u_{xxt}(l,t)] = m_T u_{tt}(l,t) \ , \quad t > 0
\end{aligned} \tag{9}$$

Here, note that the tip mass is present in the boundary conditions as well as the damping moment. The total damping mechanism used in (9) is the analog to proportional damping i.e., a linear combination of mass (I) and stiffness.

Time Hysteresis Hysteretic damping terms are most commonly associated with sinusoidal loadings. The generic idea of including a mechanism in the beam vibration constitutive equation indicating that stress is proportional to strain plus the past history of the strain can be accomplished by introducing an integral term of the form

$$\int_{-\gamma}^{0} g(s) u_{xx}(x,t+s)\,ds \tag{10}$$

where the history kernel $g(s)$ is defined by

$$g(s) = \frac{\alpha e^{\beta s}}{\sqrt{-s}} \tag{11}$$

where α and β are constants. Since the introduction of the heredity integral occurs in the stress strain relationship, the boundary conditions must also be modified. In this case the boundary value problem of interest becomes

$$\rho u_{tt}(x,t) + \frac{\partial^2}{\partial x^2}\left[EIu_{xx} - \int_{-\gamma}^{0} g(s)u_{xx}(x,t+s)ds \right] = f(t,x)\ ,\ x\in(0,1),\ t>0$$
$$u(0,t) = u_x(0,t) = 0 \qquad t>0 \tag{12}$$

$$EIu_{xx}(l,t) - \int_{-\gamma}^{0} g(s)u_{xx}(l,t+s)ds = Ju_{xtt}(l,t), \qquad t>0$$
$$\frac{\partial}{\partial x}\left[EIu_{xx}(l,t) - \int_{-\gamma}^{0} g(s)u_{xx}(l,t+s)ds \right] = m_T u_{tt} \qquad t>0$$

Note again that the inclusion of a damping mechanism in the equation of motion also effects the boundary condition.

Spatial Hysteresis Another type of damping proposed by Russell[4] is based on interpreting the energy lost in the transverse vibration of a beam as resulting from differential rates of neighboring beam sections causing internal friction. This is modeled by the expression

$$\frac{\partial}{\partial x}\left[\int_0^l h(x,\xi)\{u_{xt}(t,x) - u_{xt}(t,\xi)\}d\xi \right] \tag{13}$$

where the kernel $h(x,\xi)$ is defined by

$$h(x,\xi) = \frac{a}{b\sqrt{2\pi}} e^{-(x-\xi)^2/2b^2} \tag{14}$$

Under these circumstances the equation of the beam vibration becomes

$$\rho u_{tt} + \frac{\partial^2}{\partial x^2}[EIu_{xx}] + \gamma u_t$$
$$-\frac{\partial}{\partial x}\left[\int_0^l h(x,\xi)\{u_{xt}(x,t) - u_{xt}(\xi,t)\}d\xi \right] = f(x,t),\ x\in(0,l)\ ,\quad t>0 \tag{15}$$
$$u(0,t) = u_x(0,t) = 0, \qquad t>0$$
$$EIu_{xx} = -Ju_{xtt} \qquad t>0,\ x=l$$
$$\frac{\partial}{\partial x}[EIu_{xx}] - \left[\int_0^l h(x,\xi)\{u_{xt}(x,t) - u_{xt}(\xi,t)\}dx \right] = m_T u_{tt} \qquad t>0\ ,\ x=l$$

where again the damping mechanism changes the boundary conditions.

In total the various models represented by equations (9), (12) and (15) represent four possible sources of damping presented in various combinations. The approach taken here is to attempt to fit each of the combinations of damping models listed above to experimentally measured data. By examining each model's ability to numerically reproduce measured data, a best model is chosen from these as being most representative of the cantilever quasi-isotropic beam. As is discussed in section V, these models all admit reasonable mathematical formulations.

IV. Problem Statement

The various damping coefficients introduced in the preceding discussion cannot be measured by static experiments. Thus, the damping constants γ, c_d, α, β, a, and b must all be estimated based on measurements taken from dynamic experiments. The procedure suggested here is to estimate various groups of damping parameters such as indicated in the three models of equations (9), (12) and (15). Once these coefficients are estimated they are used in the model to produce a numerical simulation of the response of the structure under consideration subjected to identical experimental inputs. The analytical time response (with the estimated coefficients) is then compared with the experimentally measured time response. The model with the damping mechanism that best agrees with (predicts) the experimental response is then considered to be a valid physical model.

In particular, several vectors of parameters, $\mathbf{q}$, are defined one for each model of interest. For the three cases discussed here they are:

$$\mathbf{q}_1 = [EI \quad c_d I \quad \gamma] \tag{16}$$

which delineates the first damping model as defined by equation (9). Here c_d is the internal strain rate damping coefficient and γ is the linear air damping coefficient. The second model considered, as defined by equation (12), is characterized by the parameter vector

$$\mathbf{q}_2 = [EI \quad \alpha \quad \beta] \tag{17}$$

where α and β characterize the time historetic damping term. The last model considered contains a combination of linear air damping, defined by the coefficient γ, and spatial hysteresis defined by the constants a and b. The parameter vector for the third system defined by equation (15) is

$$\mathbf{q}_3 = [EI \quad \gamma \quad a \quad b] \tag{18}$$

Other combinations of the four damping mechanism are possible but were dismissed as discussed in the later section on results.

Note that in each case the parameter vector contains the flexural stiffness constant EI. For most common materials EI is tested, tabulated and well known. However in this case the material is a prototype composite with unknown material properties. Thus EI is also estimated. Because of the relative size of the air damping coefficient c_d, the term $c_d I$ is estimated.

V. Results

First the problem $\mathbf{q}_1$ is addressed by experimental modal analysis methods. In this case the coefficients of $\mathbf{q}_1$ are estimated by fitting the parameters of $\mathbf{q}_1$ to the measured damping ratios, ζ_n and natural frequencies ω_n^2 using least squares. The results given by Cudney and Inman[5] illustrate clearly that the air damping dominates the dissipation in the lower modes while strain rate damping dominates the response in higher modes. The modal model, which depends on knowing the analytical expression for the systems eigenvalues (of a cantileverd beam in this case) give consistent results in a frequency range of up to 750 Hz.

The modal equations for the problem $\mathbf{q}_1$ are given by

$$\ddot{a}_n(t) + \left(\frac{\gamma}{\rho A} + \frac{c_d I}{\rho A} \beta_n^4 \right) \dot{a}_n(t) + \frac{EI}{\rho A} \beta_n^4 a_n(t) = f_n(t) \tag{19}$$

where β_n^4 are the eigenvalues of the stiffness operator with respect to the appropriate boundary conditions and must be known analytically for the modal approach to work. The coefficients of

$a_n(t)$ and $\dot{a}_n(t)$ are compared with the measured modal damping ratios $\hat{\zeta}_n$, and natural frequencies, $\hat{\omega}_n^2$. A least squares fit is then made between the measured modal data and the analytical coefficients using

$$\beta_n^4 \frac{EI}{\rho A} = \hat{\omega}_n^2 \quad \text{and} \quad \frac{\gamma}{\rho A} + \frac{c_d I}{\rho A}\beta_n^4 = 2\hat{\zeta}_n \hat{\omega}_n \tag{20}$$

The results for a number of impact tests are given in figures 1 and 2.

Table 1 lists the analytical expressions used for the eigenvalues β_i for the first 9 modes as tabulated by Gorman for the beam parameters given in table 2. Figure 1 illustrates the modal estimate of the elastic modulus which is basically constant at $E = 2.68 \times 10^{10}$N/m^2 with a variance of 6N/m^2. Figure 2 illustrates the consistency of the damping estimates over the mode number for a weighted least squares fit to equation (20). Reference 5 contains the details. The dashed line indicates the analytically determined damping coefficient $2\zeta_n\omega_n$, based on the estimate of γ (= 1.75 N-sec/m^2) and c_d (= 20,500 N-sec/m^2), versus mode number (1-9). The solid line corresponds to the measured values $2\hat{\zeta}_n \hat{\omega}_n$ versus mode number. The results are fairly consistent, however not in exact agreement. The disagreement motivates the search for a more exotic damping mechanism such as the hysteresis term considered next.

Note that solving the second of equations (20) for the damping ratio ζ_n yields

$$\zeta_n = \frac{\gamma}{2\omega_n} + \frac{c_d}{2E^2 I}\omega_n \tag{21}$$

This states explicitly that the viscous air damping (external) is most dominate at the lowest modes, n = 1, 2, and that the strain rate (internal) damping mechanism dominates the decay rate at the higher modes. This agrees with physically intuitive notion that the low frequency modes are pushing more air than the higher frequency, lower amplitude modes. In fact, for a free-free configuration it is claimed by Vinson[6] that this effect can be subtracted.

The modal approach is not capable of examining hysteresis effects. Hence, spline inverse procedures are used. These time domain procedures are not limited to modal damping ratios or assumptions of time invariance and allow for spatially varying coefficients. Hence, they are used to estimate and compare the three models suggested in section IV. This procedure, described in Reference 7, uses cubic spline approximations to each set of differential equations and forms a sequence of least squares problems minimizing the difference between the analytical and experimental accelerations (for velocities, if so desired). The sequence converges to the best value of q for a given set of data. The functionals minimized are of the form

$$J^N(\mathbf{q}) = \Sigma |u_{tt}^N(t_i, x_j, \mathbf{q}) - \hat{u}_{tt}(t_i, x_j)|^2 \tag{22}$$

where $\hat{u}$ denotes measurements at time t_i and point x_j (at the tip in many cases), and where the summation is over the number of discrete time measurement, i. The superscript N denotes the order of each term of the sequence of approximations as discussed in Reference 7.

Problem $\mathbf{q}_1$ was solved again using a slightly more complicated cantilevered beam with a tip mass. The stiffness parameter (elastic modulus) E was estimated to be 2.71 x 10^{10}N/m^2, in good agreement with the modal estimation results above. Estimates of air damping by itself or strain rate by itself proved to be inadequate in reproducing time histories matching those of the experimental data, indicating a poor model. The difference between the numerical solution for the time history of the acceleration $u_{tt}(x_i,t)$ for the analytical model with the estimated parameter $\mathbf{q}_1$ and the experimentally measured accelerations define the residual which is generally small.[8] The analytical time response is plotted along with the measured time response versus time in figure 3. While the agreement is fair, the residual is larger for some time intervals, warranting further modeling.

Next, the temporal hysteresis model $\mathbf{q}_2$ is considered as a possible candidate for modeling the damping in the composite. In this case, the estimation procedure produces (i.e., consistent with our previous methods for estimating $\mathbf{q}_1$) a good value for E but drives the air damping coefficient to zero. The residual, however, is better than that for model $\mathbf{q}_1$. Figure 4 illustrates a plot of the measured acceleration versus time as well as the acceleration predicted by the estimate. The difference between the measured and predicted value of the time interval of interest is almost negligible. Because this model drives the air damping coefficient to zero violating physical intuition, a third model ($\mathbf{q}_3$) was considered.

The last model considered is based on a concept of spatial hysteresis as defined by problem $\mathbf{q}_3$. Again the resulting estimate of the elastic modulus E is consistent with those estimated previously. The values estimated for the spatial hysteresis (a = 1.040394, b = 0.064362) and air damping coefficient (γ = .090189) produce an excellent match between predicted and measured response as indicated[9] in figure 4. However, the external damping coefficient γ, differs from that estimate by the $\mathbf{q}_1$ model (γ = .0315).

VI. Conclusion and Discussion

Three different models of damping have been presented to account for the experimentally description observed dissipation in a composite beam. A spline based inverse procedure (SIP) which relies on the distributed parameter nature of the damping mass and stiffness parameters was used to estimate the form of the proposed damping mechanism. External air damping, strain rate damping, spatial hysteresis and time hysteresis models were considered. The spline based method was also compared to a standing experimental modal analysis (EMA) approach. The EMA approach is not applicable to the various hysteresis models, nor is it applicable to systems with spatially varying parameters in general. Both the SIP and EMA approaches yield consistent values for the elastic modulus (E) for all three estimations models. This is consistent with the fact that frequencies are much more robust to estimate than damping quantities are. Both hysteresis models produce better results than the strain rate damping mode. However, the spatial hysteresis model allows for the air damping term which time hysteresis does not. Since air damping is obviously present the time hysteresis result is less satisfying. A comparison of the hysteresis models is given in reference 9. However, the physical explanation of spatial hysteresis is equally unsatisfying. Hence, further analysis and modeling is required before a critical decision can be made among the various models.

VII. Acknowledgements

This research was supported in part under the following grants and contracts: NASA: MSM-8351807 (DJI) and several DOD equipment grants: AFOSR: 85-0119,87-0099 (DJI). The author also wishes to acknowledge H.H. Cudney, R.H. Fabiano, H. Ito, I.G. Rosen, D.L. Russell and Y. Wang for their comments, suggestions and data.

VIII. References

1. Wilson, M.L. and Miserentino, R, "Pultrusion Processes Development for Long Space Boom Models," Proceedings of the 41st Annual Conference of the Reinforced Plastics/Composites Industry, Paper #6-D, 1986.
2. Clough, R.W. and Penzion, J, *Dynamics of Structures*, John Wiley and Sons, New York, NY, 1975.
3. Inman, D.J., *Vibration with Control, Measurement and Stability*, Prentice Hall, Englewood Cliffs, NJ, 1989.
4. Russell, D.L., "On Mathematical Models for the Elastic Beam with Frequency Proportional Damping," *Control and Estimation in Distributed Parameter Systems*, SIAM, to appear.
5. Cudney, H.H. and Inman, D.J., "Experimental Verification of Damping Mechanisms in a Composite Beam," Proceedings of the 7th International Modal Analysis Conference, pp. 1989.
6. Spirnak, G.T.and Vinson, J.R., "The Effect of Temperature on the Material Damping of Graphite;Epoxy Composites in a Simulated Space Environment," *Recent Advances in the Macro-Micro-Mechanics of Composite Materials and Structures*, AD- Vol. 4, ASME, pp. 189-192, 1988.
7. Banks, H.T., Crowley, J.M. and Rosen, I.G., "Methods for the Identification of Material Parameters in Distributed Models for Flexible Structures," *Mathematical Applications and Computations*, Vol. 5, pp. 139-168, 1986.
8. Banks, H.T., Wang, Y., Inman, D.J. and Cudney, H.H., "Parameter Identification Techniques for the Estimation of Damping in Flexible Structures Experiments," Proceedings of the 26th IEEE Conference on Decision and Control, Vol. 2, 1987, pp. 1392-1395.
9. Banks, H.T., Fabiano, R.H., Wang, Y., Inman, D.J. and Cudney, H.H., "Spatial Versus Time Hysteresis in Damping Mechanisms," Proceedings of the 27th IEEE Conference on Decision and Control, pp. 1674-1677, 1988.

Table 1. Theoretical eigenvalues of a clamped-free beam.

Mode Number	Eigenvalue (β_i)
1	1.875
2	4.694
3	7.855
4	10.996
5	14.137
6	17.279
7	20.420
8	23.562
9	26.704

Table 2. Beam parameters.

Length (meters) (l)	1.0
Moment of Inertia (meter^4) (I)	1.64×10^{-9}
Density (kilograms/meter^3) (ρ)	1710
Area, cross section (meter^3) (A)	0.597×10^{-3}

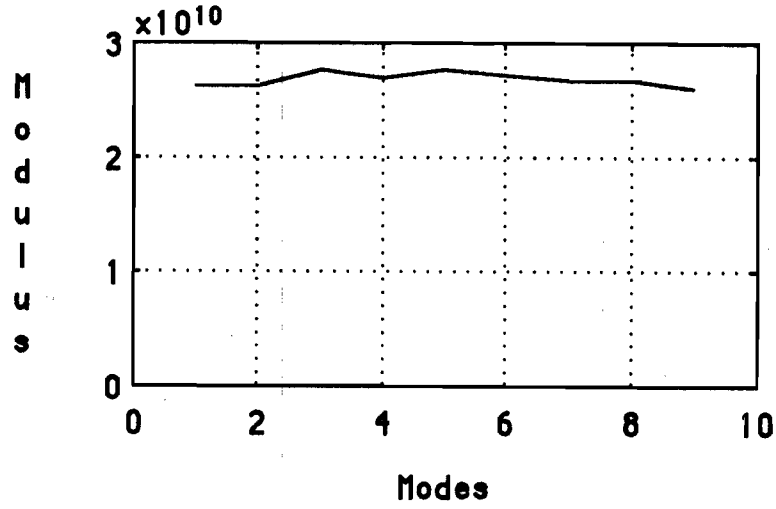

Figure 1. Estimated Youngs' modulus (N/m^2) for each mode.

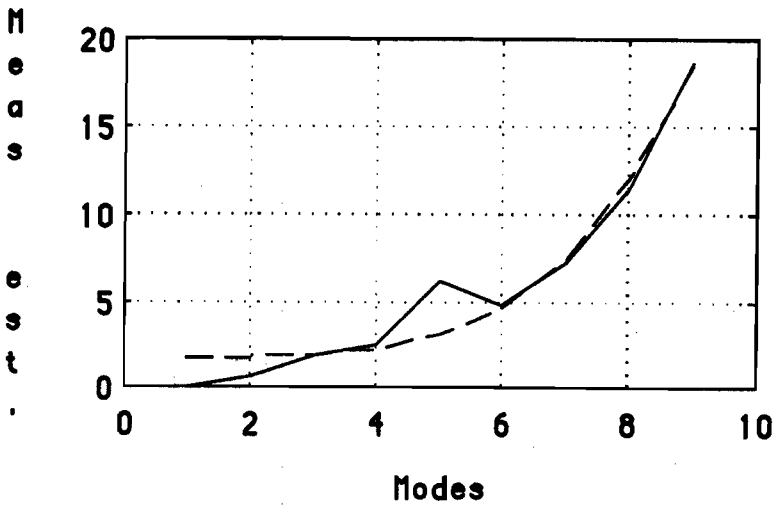

Figure 2. Measured modal parameters, $2\zeta_n\omega_n$ (solid line) and $\frac{1}{\rho A}\gamma + \frac{\beta_i I}{\rho A} c_d$ (dashed line) for each mode ($N\text{-}sec/m^2$).

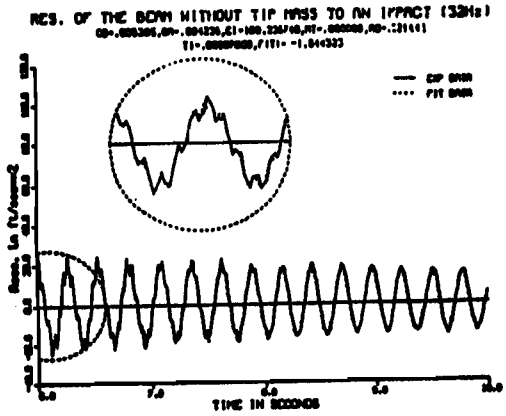

Figure 3. A comparison of the experimentally measured time response and model q_1.

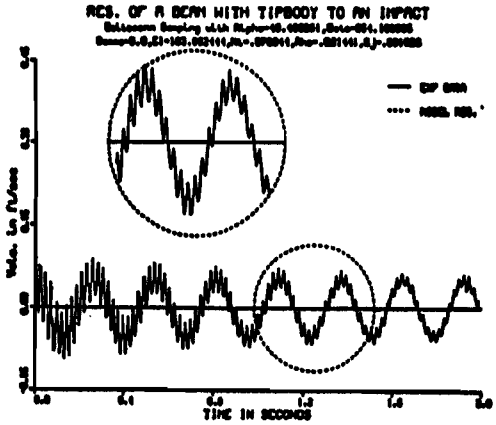

Figure 4. A comparison of the experimentally measured time response and model q_2.

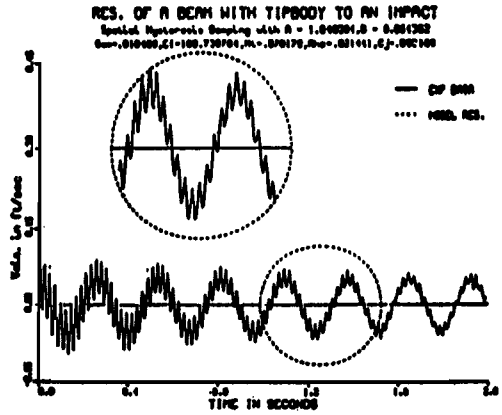

Figure 5. A comparison of the experimentally measured time response and model q_3.